Finite Bubble Statistics Constrain Late Cosmological Phase Transitions

Gilly Elor,[1] Ryusuke Jinno,[2,3] Soubhik Kumar,[4,5,6] Robert McGehee,[7,8] and Yuhsin Tsai[9]
[1]Weinberg Institute, Department of Physics, University of Texas at Austin, Austin, Texas 78712, USA
[2]Research Center for the Early Universe (RESCEU), Graduate School of Science, The University of Tokyo, Tokyo 113-0033, Japan
[3]Department of Physics, Graduate School of Science, Kobe University, 1-1 Rokkodai, Kobe, Hyogo 657-8501, Japan
[4]Center for Cosmology and Particle Physics, Department of Physics, New York University, New York, New York 10003, USA
[5]Berkeley Center for Theoretical Physics, Department of Physics, University of California, Berkeley, California 94720, USA
[6]Theoretical Physics Group, Lawrence Berkeley National Laboratory, Berkeley, California 94720, USA
[7]William I. Fine Theoretical Physics Institute, School of Physics and Astronomy, University of Minnesota, Minneapolis, Minnesota 55455, USA
[8]Leinweber Center for Theoretical Physics, Department of Physics, University of Michigan, Ann Arbor, Michigan 48109, USA
[9]Department of Physics, University of Notre Dame, Indiana 46556, USA

(Received 10 January 2024; revised 1 July 2024; accepted 10 October 2024; published 20 November 2024)

We consider first order cosmological phase transitions (PTs) happening at late times below standard model temperatures $T_{\rm PT} \lesssim$ GeV. The inherently stochastic nature of bubble nucleation and the finite number of bubbles associated with a late-time PT lead to superhorizon fluctuations in the PT completion time. We compute how such fluctuations eventually source curvature fluctuations with universal properties, independent of the microphysics of the PT dynamics. Using cosmic microwave background (CMB) and large scale structure measurements, we constrain the energy released in a dark-sector PT. For 0.1 eV $\lesssim T_{\rm PT} \lesssim$ keV this constraint is stronger than both the current bound from additional neutrino species $\Delta N_{\rm eff}$, and in some cases, even CMB-S4 projections. Future measurements of CMB spectral distortions and pulsar timing arrays will also provide competitive sensitivity for keV $\lesssim T_{\rm PT} \lesssim$ GeV.

DOI: 10.1103/PhysRevLett.133.211003

Phase transitions (PTs) have been studied extensively for decades in models of baryogenesis [1–4], (asymmetric) dark matter [5–13], extended Higgs sectors [14–17], and spontaneously broken conformal symmetry [18–28], among others. PTs may also generate gravitational waves (GWs) [29–36] that can be observed in the near future.

"Late-time" PTs have garnered attention due to their possible connections to puzzling observations from pulsar timing arrays (PTAs) [37,38] and the "H_0 tension": a discrepancy between the direct measurements of the Hubble constant H_0 [39] and its value inferred from the cosmic microwave background (CMB) [40] (for a review see [41]). These PTs occur below standard model (SM) temperatures of a GeV (redshift $z \sim 10^{13}$) and before matter-radiation equality ($z \approx 3400$). For instance, a PT around $z \approx 10^4$ is motivated by the proposed new early dark energy (NEDE) solution to the H_0 problem [42–46]. Since the Hubble tension favors such "early-time" solutions [47], other ideas also use such PTs [48,49]. A PT at $z \sim 10^{10}$ has also been proposed as a source of the observed stochastic GW background measured by PTAs [37,50–53]. Even later PTs may ameliorate the cosmological constant problem [54].

Because of constraints from big-bang nucleosynthesis and the CMB, late-time PTs that occur entirely in a dark sector with no significant reheating to SM particles are favored [55]. Thus, we focus on PTs that only release GWs and other forms of dark radiation (DR). The gravitational backreaction on the SM sector is the only way to identify and constrain such dark-sector PTs. For nongravitational couplings between the dark sector and SM, stronger constraints than the "model-independent" constraints that we derive in this work could apply. A well-known constraint on post-big-bang nucleosynthesis dark PTs is the bound on the number of additional neutrinos, $\Delta N_{\rm eff} < 0.29$ at 95% CL [40,56], derived from baryon acoustic oscillation (BAO) and CMB measurements. This places an upper bound on the fraction of DR energy density compared to the total radiation energy density $f_{\rm DR} \equiv \rho_{\rm DR}/\rho_{\rm tot} \lesssim 0.04$.

A PT proceeds via nucleation of bubbles of true vacuum inside the metastable phase. To estimate the typical number of bubbles, consider a comoving volume corresponding to an angular scale $\sim 10^{-3}$ radian, the current CMB resolution. If $T_{\rm PT} \sim$ TeV, there are an enormous number of bubbles

inside that comoving volume: $N_b \sim [a(\mathrm{TeV})H(\mathrm{TeV})/(10^3 a_0 H_0)]^3 \sim \{\tau_0/[10^3\tau(\mathrm{TeV})]\}^3 \sim 10^{34}$. Here, $\tau(\mathrm{TeV})$ and τ_0 are the conformal times at $T = \mathrm{TeV}$ and today, respectively, with the corresponding scale factors denoted by $a(\mathrm{TeV})$ and a_0. However, if $T_{\mathrm{PT}} \sim \mathrm{keV}$, for example, the number of bubbles is much less, $N_b \sim 10^6$.

In this Letter, we demonstrate that the finite number of bubbles involved in a PT gives rise to superhorizon perturbations in PT completion time $\propto 1/\sqrt{N_b}$ that eventually contribute to curvature perturbations. This means for $T_{\mathrm{PT}} \sim \mathrm{TeV}$, the finite number contribution $1/\sqrt{N_b} \sim 10^{-17}$ is negligible when compared to the standard inflationary fluctuation $\sim 10^{-5}$. However, for $T_{\mathrm{PT}} \sim \mathrm{keV}$, the finite number contribution $\sim 10^{-3}$ is relevant. We present the first calculation of these perturbations using gauge-invariant observables and show that on large length scales these perturbations follow a universal power-law scaling in the PT parameters, independent of its microscopic details [57]. Even for a dark sector with no direct coupling to the SM, CMB, and large scale structure () measurements constrain the resulting curvature perturbations. This in turn constrains f_{DR} more strongly than the current and projected ΔN_{eff} limits when $T_{\mathrm{PT}} \lesssim 1$ keV. Additionally, the power-law scale dependence of this new contribution to curvature perturbations can create distinct signatures in the CMB and matter power spectrum, enabling us to identify the origin of the perturbation as a late-time PT.

Superhorizon fluctuations in percolation time from number of bubbles—A PT proceeds through bubble nucleation and expansion; a point in space transitions to the true vacuum when a bubble engulfs it. However, this process is inherently *stochastic*, and therefore, not all points in space transition to the true vacuum at the same time. To quantify this, we can write the fraction of space in the false vacuum as a function of time (ignoring space-time expansion; see [63] for a recent review) as

$$P_f(t) = \exp\left(-\int_{t_0}^{t} \mathrm{d}t' \Gamma(t') V(t,t')\right), \tag{1}$$

where t_0 denotes the start of the PT and $V(t,t')$ is the fractional volume of bubbles at time t after being nucleated at time t'. The nucleation rate $\Gamma(t)$ can be written [63–66], with $\beta = -S'(t_f)$ and bounce action $S(t)$ parametrizing the tunneling rate, as

$$\Gamma = \Gamma_0 e^{-S(t)} \approx \Gamma_0 e^{-S(t_f)} e^{\beta(t-t_f)}. \tag{2}$$

This shows that the false vacuum fraction drops exponentially as Γ increases as $t \to t_f$ and the PT completes. The timescale t_f, conventionally defined by when $P_f(t_f) = 1/e$ [63], is roughly the Hubble time H_{PT}^{-1} at T_{PT}. For our perturbation studies, the more relevant timescale is the duration $t = [t_f - \beta^{-1}, t_f]$, during which Γ grows significantly, completing the PT. This PT duration β^{-1} sets the bubble expansion time window, making the average bubble size right before the PT completes $d_b \approx (8\pi)^{1/3} v_w/\beta$ [65,66], with v_w as the bubble wall velocity. Additionally, the perturbation of the PT time is expected to be of the order of the PT duration $\sim\beta^{-1}$, meaning a smaller β results in a larger variation.

To characterize the variation in the PT completion time, we denote the time at which a point $\vec{x}$ transitions to true vacuum by $t_c(\vec{x})$, and compute the two-point function $\mathcal{P}_{\delta t} \equiv H_{\mathrm{PT}}^2 \langle \delta t_c(\vec{x}) \delta t_c(\vec{y})\rangle$. Here, $\delta t_c(\vec{x}) = t_c(\vec{x}) - \bar{t}_c$ with $\bar{t}_c \approx t_f \approx 1/(2H_{\mathrm{PT}})$, the average time of conversion. Practically, it is easier to write $\mathcal{P}_{\delta t} = (H_{\mathrm{PT}}/\beta)^2 \times \beta^2 \langle \delta t_c(\vec{x}) \delta t_c(\vec{y})\rangle$ and calculate the last factor, thus separating the effect of cosmic expansion from the PT dynamics. We can quantify the perturbation with the dimensionless Fourier transformed two-point function denoted by

$$\mathcal{P}_{\delta t}(k) = \frac{k^3}{2\pi^2}\left(\frac{H_{\mathrm{PT}}}{\beta}\right)^2 \int \mathrm{d}^3 r\, e^{i\vec{k}\cdot\vec{r}} \beta^2 \langle \delta t_c(\vec{x}) \delta t_c(\vec{y})\rangle, \tag{3}$$

where $\vec{r} = \vec{x} - \vec{y}$. This characterizes the correlation of t_c between any two points separated by a distance $\sim 1/k$.

$\mathcal{P}_{\delta t}(k)$ changes qualitatively for modes smaller or larger than the typical bubble size $\sim v_w/\beta$. For k modes smaller than or comparable to the bubble size, we can analytically compute $\mathcal{P}_{\delta t}(k)$. However, due to intricate fluid dynamics and magnetohydrodynamics effects, a translation between $\mathcal{P}_{\delta t}(k)$ and sourced curvature perturbations is involved and model-dependent. Therefore, the dependence of the curvature power spectrum on k for $k_p \equiv k/a_{\mathrm{PT}} \gtrsim \beta/v_w$ is less universal and varies as the properties of the PT change. (Here, k_p is a physical wave number and a_{PT} is the scale factor at t_f.) On the other hand, scales $k_p \ll \beta/v_w$ have many bubbles contributing to the correlation function within a spatial volume of linear size $1/k_p$. Thus, $\mathcal{P}_{\delta t}$ is more universal and less sensitive to the details of the PT thanks to the central limit theorem.

We can understand the behavior of $\mathcal{P}_{\delta t}$ for $k_p \ll \beta/v_w$ as follows. In a given volume V, there are $N \sim V/d_b^3$ independent regions where bubble nucleation can take place in an uncorrelated fashion. As a result, the standard deviation in PT completion time, when averaged over this entire volume, scales as $1/\sqrt{N}$. Thus, given $N \sim 1/(k_p d_b)^3$ for a scale k_p, we expect $\mathcal{P}_{\delta t} \propto (k_p d_b)^3$. Also, the combination $\beta \times t$ is what appears in the nucleation rates in Eqs. (2) and (1), so $\mathcal{P}_{\delta t} \propto 1/\beta^2$. Thus, for $k_p \ll \beta/v_w$ and $H_{\mathrm{PT}} \ll \beta$, the dimensionless power spectrum scales as

$$\mathcal{P}_{\delta t} \sim 8\pi \left(\frac{H_{\mathrm{PT}}}{\beta}\right)^2 \left(\frac{v_w k_p}{\beta}\right)^3 = 8\pi c v_w^3 (k\tau_*)^3 \left(\frac{H_{\mathrm{PT}}}{\beta}\right)^5, \tag{4}$$

with $\tau_* = 1/(a_{\mathrm{PT}} H_{\mathrm{PT}})$ for PTs during radiation domination and a constant prefactor c. From the qualitative arguments above we expect $c \sim 1$; a detailed calculation in the Supplemental Material [67] gives $c \approx 2.8$, which is what we use to derive the constraints below. Another way to

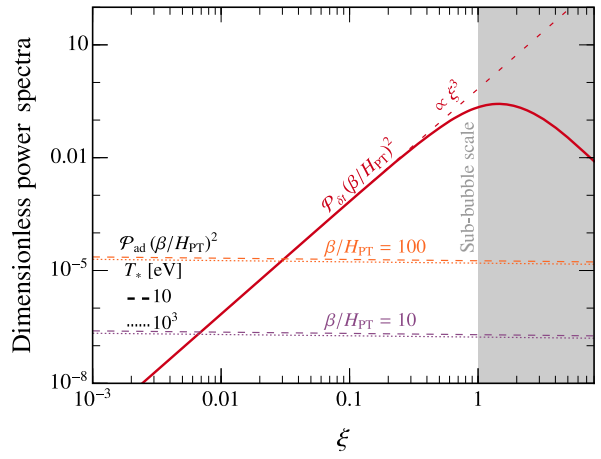

FIG. 1. Dimensionless power spectrum of phase transition time fluctuation, rescaled by $(\beta/H_{\rm PT})^2$ and plotted against comoving wave number ratio ξ representing the perturbation mode relative to typical bubble separation. The PT spectrum (red) derived in the Supplemental Material is independent of $(\beta, \tau_{\rm PT})$, unlike adiabatic perturbations (purple, orange).

understand the same k^3 scaling of $\mathcal{P}_{\delta t}$ for small k is through Eq. (3). We show in the Supplemental Material that the correlation $\langle \delta t_c(\vec{x}) \delta t_c(\vec{y}) \rangle \sim e^{-\beta r a_{\rm PT}/2}$ for $\beta r a_{\rm PT} \gg 1$. As a result for $k_p \ll \beta/v_w$, the exponential phase in Eq. (3) does not contribute, and the k dependence of $\mathcal{P}_{\delta t}$ comes solely from the k^3 prefactor. A similar dependence arises in the context of primordial black holes, as studied in [70,71].

The result for $\mathcal{P}_{\delta t}$ is in Fig. 1, where $\xi \equiv k_p d_b = (8\pi)^{1/3} v_w (k\tau_{\rm PT})(H_{\rm PT}/\beta)$. For $\xi \ll 1$, $\mathcal{P}_{\delta t} \sim \xi^3 (H_{\rm PT}/\beta)^2$, as expected from Eq. (4). However, close to $\xi \sim 1$, we see a deviation from that scaling. Below, we only use the result for $\mathcal{P}_{\delta t}$ for $\xi \leq 1$ since the regime $\xi \gg 1$ is sensitive to turbulence and magnetohydrodynamics effects. However, these subhorizon inhomogeneities also give rise to density perturbations. In dark sectors in which sound waves dominantly source the GWs, the resulting constraints may even be stronger [72].

We have described how the PT completion time fluctuates on superhorizon and "superbubble" scales. While such fluctuations are of "isocurvature" type initially (since they do not induce a change in energy density), eventually they source curvature perturbations, as we discuss now.

Curvature perturbations from fluctuations in percolation time—Consider two acausal patches, A and B, where the PT takes place. Since our analysis relies on $\xi \sim 0.1$–1 and $\beta/H_{\rm PT} \lesssim 10^3$, we are in a regime where $\mathcal{P}_{\delta t} \gg A_s$, where $A_s = 2.1 \times 10^{-9}$ [73] is the magnitude of the inflationary scalar power spectrum (we express $\mathcal{P}_{\delta t}$ in terms of gauge-invariant observables below). Thus, we can ignore effects due to A_s and assume the PT takes place in a universe that is *a priori* homogeneous in different patches. We will see how $\mathcal{P}_{\delta t}$ leads to inhomogeneities in the dark sector and how they then feed back into the SM sector, weighted by factors of $f_{\rm DR}$.

Take the two patches A and B to each have size v_w/β and equal energy density. ρ_F is their (equal) false vacuum energy density and t_c^A and t_c^B their respective PT completion times. $t_c^A \neq t_c^B$ in general and we define the difference $t_c^B - t_c^A \equiv \delta t_c \ll t_c^{A,B} \sim 1/H_{\rm PT}$, with $\delta t_c > 0$. When A and B undergo the PT, ρ_F is converted into DR with an energy density $\tilde{\rho}_{\rm DR}$ [74]. Right at t_c^A, the energy densities in A and B are identical and the curvature perturbation is still zero. However, there is a nonzero isocurvature perturbation in DR at this time. This subsequently induces curvature perturbations as time evolves since DR and vacuum energy redshift differently. In other words, the equation of state of the Universe is not barotropic, i.e., the total pressure is not a definite function of the total energy, $p \neq p(\rho)$. As a result, the curvature perturbation is not constant (see, e.g., [76,77]) and evolves with time after the PT occurs.

We can write the DR energy density in the two patches at a later time $t_{\rm fin}$ as

$$\rho_{\rm DR}^{A,B}(t_{\rm fin}) = \rho_F \left(\frac{t_c^{A,B}}{t_{\rm fin}} \right)^2 + \rho_{\rm DR'}(t_{\rm fin}). \tag{5}$$

Here, $\rho_{\rm DR'}(t_{\rm fin})$ denotes the energy density in a component of DR that does not come from the PT, and therefore is the same for both patches. This shows that the total energy densities of DR in the two patches are different and a nonzero DR density perturbation has been sourced by the DR isocurvature perturbation. (The different values of $\rho_{\rm DR}$ in A and B change Hubble in the two patches, altering the energy-density redshift, but this correction is $\mathcal{O}(\delta\rho_{\rm DR}/\rho_{\rm SM})$ and negligible for our leading-order analysis.) We can compute this density perturbation using Eq. (5), $\delta\rho_{\rm DR}/\tilde{\rho}_{\rm DR} = 2\delta t_c/t_c$. Since we are working to leading order in perturbations, the DR energy density sourced from ρ_F is given by $\tilde{\rho}_{\rm DR} \equiv \rho_F (t_c/t_{\rm fin})^2$ and we use the homogeneous value of t_c here.

To compute the associated curvature perturbation, we can use the spatially flat gauge (for a review, see [78]), which amounts to comparing the energy densities in patches A and B at a common time $t_{\rm fin}$ when the scale factors are identical. Then the curvature perturbation (on uniform-density hypersurfaces) is

$$\begin{aligned} \zeta &= -\frac{H_{\rm PT}\delta\rho_{\rm DR}}{(\dot{\tilde{\rho}}_{\rm DR} + \dot{\rho}_{\rm DR'} + \dot{\rho}_{\rm SM})} = \frac{1}{4} f_{\rm DR} \frac{\tilde{\rho}_{\rm DR}}{\tilde{\rho}_{\rm DR} + \rho_{\rm DR'}} \frac{\delta\rho_{\rm DR}}{\tilde{\rho}_{\rm DR}} \\ &= \frac{1}{2} f_{\rm DR} \left(\frac{\alpha_{\rm PT}}{1+\alpha_{\rm PT}} \right) \frac{\delta t_c}{t_c} = f_{\rm DR} \left(\frac{\alpha_{\rm PT}}{1+\alpha_{\rm PT}} \right) H_{\rm PT} \delta t_c. \end{aligned} \tag{6}$$

Here, we have used the notation $\alpha_{\rm PT} = \tilde{\rho}_{\rm DR}/\rho_{\rm DR'}$ and $f_{\rm DR} = (\tilde{\rho}_{\rm DR} + \rho_{\rm DR'})/(\tilde{\rho}_{\rm DR} + \rho_{\rm DR'} + \rho_{\rm SM})$. In terms of this the curvature power spectrum is given by

$$\mathcal{P}_\zeta(k) = f_{\rm DR}^2 \left(\frac{\alpha_{\rm PT}}{1+\alpha_{\rm PT}} \right)^2 \mathcal{P}_{\delta t}(k) + \mathcal{P}_{\rm ad}(k). \tag{7}$$

In the last term, we have reintroduced the uncorrelated adiabatic perturbation $\mathcal{P}_{\rm ad}$. We take the pivot scale $k_* = 0.05\ {\rm Mpc}^{-1}$, $A_s = 2.1 \times 10^{-9}$, and tilt $n_s = 0.966$ [40] when calculating $\mathcal{P}_{\rm ad}$. The constraints on $\mathcal{P}_\zeta(k)$ can then be used to bound $f_{\rm DR}$ for different dark PT parameters. For an alternate derivation that relates $\mathcal{P}_{\delta t}$ to $\mathcal{P}_\zeta$ without relying on the separate universe approach followed here, together with a derivation using the δN formalism [79]; see the Supplemental Material.

Since we ignored the presence of inflationary, adiabatic perturbations while analyzing $\mathcal{P}_{\delta t}$, Eq. (7) is valid only for $\mathcal{P}_{\delta t} \gg \mathcal{P}_{\rm ad}$. In practice, given the current precision $\Delta\mathcal{P}_\zeta/\mathcal{P}_\zeta \sim 5\%$ on CMB scales, the above restriction puts an upper bound $f_{\rm DR} \lesssim 0.4$, above which the effects of A_s would be relevant for determining $\mathcal{P}_{\delta t}$. Once the PT ends, all the dominant energy densities are in radiation, and superhorizon ζ modes remain constant until they enter the horizon. We note that PT also generates DR isocurvature, with a size roughly given by $\mathcal{P}_{\delta t}$, implying that isocurvature vanishes in the limit of $\mathcal{P}_{\delta t} \to 0$. The Planck constraint on DR isocurvature [80] is similar to the constraints on curvature perturbation. Therefore, we will not consider the effect of isocurvature perturbations separately, but rather study the their effects via the constraints on $\mathcal{P}_\zeta$.

Time evolution of curvature perturbations—Perturbation modes with $k\tau_{\rm PT} \ll 1$ are outside the horizon when the PT takes place and we can characterize their subsequent cosmological evolution by just specifying $\mathcal{P}_\zeta(k)$. However, modes with $\xi \approx 1$ correspond to $k\tau_{\rm PT} \approx (8\pi)^{-1/3}(\beta/H_{\rm PT}) \times v_w^{-1} \gtrsim 1$ for $\beta/H_{\rm PT} \gtrsim 10$, implying such modes are already inside the horizon when the PT takes place. To derive constraints based on $\mathcal{P}_\zeta(k)$ for a subhorizon k mode, we need to take into account that there is no subhorizon evolution for a time $\Delta\tau \sim \tau_{\rm PT} - k^{-1}$ between mode reentry and the PT.

CMB temperature perturbations undergo diffusion damping while inside the horizon. A delay in subhorizon evolution by an amount $\Delta\tau$ implies PT-induced perturbations undergo less damping for a given k compared to lambda cold dark matter (ΛCDM) model expectations. Starting with the same value of $\mathcal{P}_\zeta(k)$, the CMB anisotropies are larger in the PT scenario compared to ΛCDM. In this Letter, we take a conservative approach by not including this enhancement and leave a more precise computation for future work.

Perturbations in dark matter experience logarithmic growth in the radiation-dominated era upon horizon reentry. In ΛCDM cosmology, the power in a k mode at the time of matter-radiation equality ($\tau_{\rm eq} \approx 110$ Mpc) is $\Delta_{\rm DM}(1/k, \tau_{\rm eq})^2 \mathcal{P}_\zeta(k)$, where $\Delta_{\rm DM}$ denotes the matter transfer function $\Delta_{\rm DM}(\tau_i, \tau) \approx 6.4 \ln(0.44\tau/\tau_i)$ [81,82]. For the PT scenario, the analogous expression is $\Delta_{\rm DM}(\tau_{\rm PT}, \tau_{\rm eq})^2 \mathcal{P}_\zeta(k)$. We use a rescaled and weaker constraint $\mathcal{P}_\zeta(k) \times [\Delta_{\rm DM}(\tau_{\rm PT}, \tau_{\rm eq})/\Delta_{\rm DM}(1/k, \tau_{\rm eq})]^2$ for $k > \tau_{\rm PT}^{-1}$ to take into account dark matter clustering bounds such as from Lyman-α (Ly-α) and future PTA constraint on dark matter clustering.

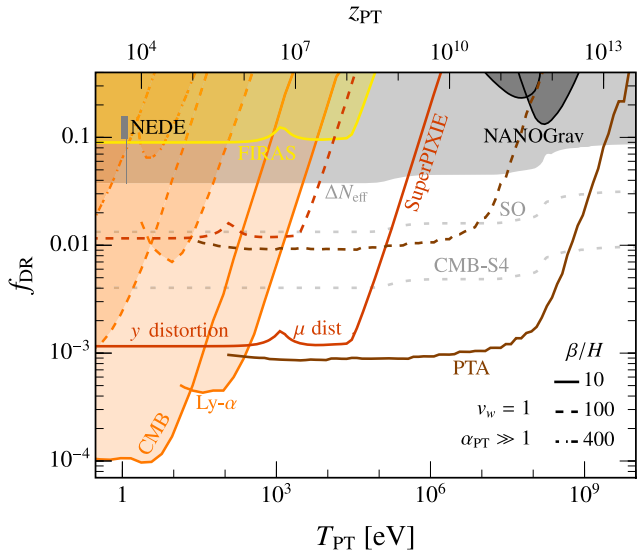

FIG. 2. 2σ exclusion bounds on DR energy density fraction from current observations, as derived in this work. We show bounds using the CMB (Planck 2018 [73]) and Ly-α [83] (orange), as well as the FIRAS constraint [86] (yellow). The light gray region represents the existing bound $\Delta N_{\rm eff} \geq 0.29$ [40], and the dotted gray lines, the projected bounds from the Simons Observatory (SO) $\Delta N_{\rm eff} \geq 0.1$ [87] and CMB-S4 $\Delta N_{\rm eff} \geq 0.03$ [88]. Future projections from SuperPIXIE [89] (red), assuming sensitivity of $\Delta\rho_\gamma/\rho_\gamma \sim 10^{-8}$, and PTA [90] (maroon) are also depicted. We display the NEDE model's preferred region [46] (darker gray) and the PT generating the potential stochastic GW background [50]. To assess existing NEDE model bounds, focus on $\beta/H_{\rm PT}$ values within the indicated bounds and disregard the gray region representing the $\Delta N_{\rm eff}$ bound.

Cosmological constraints—In Fig. 2, we present 2σ exclusion bounds on $f_{\rm DR}$ using current constraints on $\mathcal{P}_\zeta$ and projected future sensitivities. We translate the comoving time $\tau_{\rm PT}$ in Eq. (4) into the SM temperature and redshift at the time of the PT. CMB [73] and Ly-α [83] measurements set upper bounds on $\mathcal{P}_\zeta$ for k modes up to $k \lesssim 3\ {\rm Mpc}^{-1}$. Our analysis excludes the pumpkin orange regions for various $\beta/H_{\rm PT}$ since in those regions, the PT contribution to $\mathcal{P}_\zeta$ is too large. Other constraints from ultracompact minihalos impacting PTAs may be relevant for $T_{\rm PT} \gtrsim 1$ MeV, but have unknown uncertainties related to the time of dark matter collapse [84,85].

The $T_{\rm PT}$ dependence of the constraints in Fig. 2 can be understood as follows. During a radiation-dominated epoch, $k_{\rm peak} \propto T_{\rm PT}$, where $k_{\rm peak}$ is the comoving wave number of the peak in $\mathcal{P}_{\delta t}(k)$. The constraint on $f_{\rm DR}$ for a given $T_{\rm PT}$ then depends on whether $k_{\rm peak}$ or the IR tail of $\mathcal{P}_{\delta t}(k)$ lies within the range probed by a given observable. Suppose that for a range of $T_{\rm PT}$, the corresponding range of $k_{\rm peak}$ is directly constrained by an observable. Then if the

constraint on $\mathcal{P}_\zeta(k)$ over that range of $k_{\rm peak}$ is flat, the associated constraint on $f_{\rm DR}$ is also flat with respect to $T_{\rm PT}$, resulting in the plateaus in Fig. 2. This is because $\mathcal{P}_{\delta t}(k_{\rm peak})$ does not change as $T_{\rm PT}$ varies. This is what happens for the CMB bound for $T_{\rm PT} \lesssim 1$ eV for $\beta/H_{\rm PT} = 10$. For larger $T_{\rm PT}$, $k_{\rm peak}$ lies outside the region probed by $\mathcal{P}_\zeta(k)$ constraints; constraints are only sensitive to the tail of the $\mathcal{P}_{\delta t}$ distribution and $\propto f_{\rm DR}^2 k^3$ [from (4) and (7)]. In those regions, as $T_{\rm PT}$ is increased, the bound on $f_{\rm DR}$ goes as $1/T_{\rm PT}^{3/2}$ (since $T_{\rm PT} \propto k$). A similar transition from a plateau behavior is also seen at $\sim$100 eV for Ly-α and at $\sim$100 MeV for PTA.

Notably, for $\beta/H_{\rm PT} \lesssim 400$, the bounds we derive from DR inhomogeneities are stronger than current $\Delta N_{\rm eff}$ constraints that track the homogeneous abundance of DR. For PTs that occur before big-bang nucleosynthesis, there is a stricter bound of $\Delta N_{\rm eff} \lesssim 0.23$ when applying more observational constraints; for those PTs after, the constraint is slightly weaker at $\Delta N_{\rm eff} \lesssim 0.31$ [91]. Since our new CMB + Ly-α bounds are in the latter range, and we want to show analogous $\Delta N_{\rm eff}$ constraints for CMB-S4, we plot Fig. 2 using the well-known $\Delta N_{\rm eff} < 0.29$ [40]. For $\beta/H_{\rm PT} \sim 10$ and $T_{\rm PT} \lesssim$ keV, our analysis using CMB + Ly-α constrains such PTs as much as or better than the future Simons Observatory (SO) [87] and CMB-S4 projections on $\Delta N_{\rm eff}$ [88].

The NEDE model in [45,46] favors $\alpha_{\rm PT} f_{\rm DR}$ in the upper (lower) dark gray region ($\pm 1\sigma$) from the Planck18 + BAO + LSS fit with (without) SH0ES data. While large values of $\beta/H_{\rm PT}$ generally require extra model building, the model in [46] assumes $\beta/H_{\rm PT} \gtrsim 100$ and permits $\beta/H_{\rm PT}$ as large as $\sim 10^3$ by including a field to trigger the PT. Still, our $\mathcal{P}_\zeta$ bound effectively disfavors the preferred NEDE region in $(T_{\rm PT}, f_{\rm DR})$ for all values of $\beta/H_{\rm PT} \lesssim 320$ (230) with (without) SH0ES data.

For a large $\mathcal{P}_\zeta(k)$ with $k \lesssim 5400\ {\rm Mpc}^{-1}$ the PT can impact the dissipation of acoustic modes in photon-baryon perturbations, altering the photon's blackbody spectrum and inducing μ and y distortions [92,93],

$$X \approx A \int_{k_{\rm min}}^{\infty} \frac{{\rm d}k}{k} \mathcal{P}_\zeta(k) \left[B e^{-\frac{k}{5400/\ {\rm Mpc}}} - C e^{-\left(\frac{k}{31.6/\ {\rm Mpc}}\right)^2} \right], \quad (8)$$

where $k_{\rm min} = 1\ {\rm Mpc}^{-1}$, $(A, B, C)_X = (2.2, 1, 1)_\mu$ and $(0.4, 0, -1)_y$. Comparing this to the FIRAS bound of $|\mu| < 9.0 \times 10^{-5}$ and $|y| < 1.5 \times 10^{-5}$ [94,95], we derive the exclusion bound labeled as "FIRAS." When lowering $T_{\rm PT}$, the y-distortion bound takes over the μ bound around $T_{\rm PT} = 10^3$ (10^2) eV for the $\beta/H_{\rm PT} = 10$ (100) case. In contrast to Ref. [60], our findings indicate that the FIRAS constraint is less stringent than the $\Delta N_{\rm eff}$ constraint, even for PT with small $\beta = 10 H_{\rm PT}$ [96].

Current $\mathcal{P}_\zeta$ measurements are less sensitive to PTs than the $\Delta N_{\rm eff}$ constraint for $T_{\rm PT} \gtrsim$ keV, but several proposed searches can constrain $\mathcal{P}_\zeta$ more powerfully and constrain weaker dark PTs. Super-PIXIE aims to measure the CMB with a sensitivity of $\Delta\rho_\gamma/\rho_\gamma \sim 10^{-8}$ [97] and the associated constraint is shown in red. PTAs can also probe $\mathcal{P}_\zeta$ by observing the phase shift in periodic pulsar signals mainly caused by the Doppler effect induced by an enhanced dark matter structure that accelerates Earth or a pulsar. The PTA sensitivity curves (maroon) use $\mathcal{P}_\zeta$ sensitivity derived in [90] that assumes 20 years of observations of 200 pulsars. This future sensitivity to PTs with $T_{\rm PT} \gtrsim$ MeV may test exotic dark matter models that rely on them [12]. Also shown is the 2σ-preferred PT region for the GW background hinted at by NANOGrav [37,50] (darker gray; see, e.g., [98] for alternative GW spectrum assumptions). At face value, this region conflicts with the $\Delta N_{\rm eff}$ constraint, but this prominent GW signal could largely originate from supermassive black hole mergers. With enhanced PTA measurements, we might still detect the PT signal within a comparable $T_{\rm PT}$ range. Then PTA measurements of $\mathcal{P}_\zeta$ could complement the GW detection.

Discussion—We have demonstrated that finite bubble statistics can lead to superhorizon fluctuations in the PT completion time, regardless of the PT details. These fluctuations source curvature perturbations that affect the CMB, LSS, and other observables. Utilizing these, we find our constraints are in tension with some of the best fit regions of the NEDE models proposed to ameliorate the Hubble tension. At superhorizon scales, the (dimensionless) power spectrum of these fluctuations has a k^3-model-independent scaling since it is just determined by Poisson statistics. This contribution makes the *total* curvature perturbation scale noninvariant. Thus, the associated CMB phenomenology shares some similarities with the scale noninvariant effects due to "primordial features" [99] produced during inflation and models with "blue-tilted" curvature perturbation [100–103].

In our analysis, we have kept the ΛCDM parameters fixed. However, given the model-independent shape, one can do a joint analysis where both dark-sector and ΛCDM parameters are varied. We have also not considered constraints from modes that are smaller than typical bubbles as those are more model-dependent. However, in the context of specific models one can obtain stronger constraints from such modes. We leave these for future work.

Acknowledgments—We thank Matthew Buckley, Zackaria Chacko, Peizhi Du, Anson Hook, Gordan Krnjaic, Toby Opferkuch, Davide Racco, Albert Stebbins, Gustavo Marques-Tavares, and Neal Weiner for helpful comments on the draft and discussions. The research of G. E. is supported by the National Science Foundation (NSF) Grant No. PHY-2210562, by a grant from University of Texas at Austin, and by a grant from the Simons Foundation. The work of R. J. is supported by JSPS KAKENHI Grant No. 23K19048. S. K. is supported

partially by the NSF Grant No. PHY-2210498 and the Simons Foundation. R. M. was supported in part by DOE Grant No. DE-SC0007859. Y. T. is supported by the NSF Grant No. PHY-2112540. R. J., S. K., R. M., and Y. T. thank the Mainz Institute for Theoretical Physics (MITP) of the Cluster of Excellence PRISMA$^+$ (project ID 39083149) for their hospitality while a portion of this work was completed. G. E., S. K., and Y. T. thank Aspen Center for Physics (supported by NSF Grant No. PHY-2210452) for their hospitality while this work was in progress.

[1] A. G. Cohen, D. B. Kaplan, and A. E. Nelson, Phys. Lett. B **245**, 561 (1990).
[2] L. Fromme, S. J. Huber, and M. Seniuch, J. High Energy Phys. 11 (2006) 038.
[3] E. Hall, T. Konstandin, R. McGehee, H. Murayama, and G. Servant, J. High Energy Phys. 04 (2020) 042.
[4] G. Elor *et al.*, in Snowmass 2021 (2022), arXiv:2203.05010.
[5] T. Cohen, D. E. Morrissey, and A. Pierce, Phys. Rev. D **78**, 111701(R) (2008).
[6] K. M. Zurek, Phys. Rep. **537**, 91 (2014).
[7] M. J. Baker and J. Kopp, Phys. Rev. Lett. **119**, 061801 (2017).
[8] E. Hall, T. Konstandin, R. McGehee, and H. Murayama, Phys. Rev. D **107**, 055011 (2023).
[9] P. Asadi, E. D. Kramer, E. Kuflik, G. W. Ridgway, T. R. Slatyer, and J. Smirnov, Phys. Rev. Lett. **127**, 211101 (2021).
[10] P. Asadi, E. D. Kramer, E. Kuflik, G. W. Ridgway, T. R. Slatyer, and J. Smirnov, Phys. Rev. D **104**, 095013 (2021).
[11] E. Hall, R. McGehee, H. Murayama, and B. Suter, Phys. Rev. D **106**, 075008 (2022).
[12] G. Elor, R. McGehee, and A. Pierce, Phys. Rev. Lett. **130**, 031803 (2023).
[13] P. Asadi *et al.*, arXiv:2203.06680.
[14] S. Profumo, M. J. Ramsey-Musolf, and G. Shaughnessy, J. High Energy Phys. 08 (2007) 010.
[15] Z. Chacko, H.-S. Goh, and R. Harnik, Phys. Rev. Lett. **96**, 231802 (2006).
[16] P. Schwaller, Phys. Rev. Lett. **115**, 181101 (2015).
[17] I. P. Ivanov, Prog. Part. Nucl. Phys. **95**, 160 (2017).
[18] P. Creminelli, A. Nicolis, and R. Rattazzi, J. High Energy Phys. 03 (2002) 051.
[19] L. Randall and G. Servant, J. High Energy Phys. 05 (2007) 054.
[20] G. Nardini, M. Quiros, and A. Wulzer, J. High Energy Phys. 09 (2007) 077.
[21] T. Konstandin, G. Nardini, and M. Quiros, Phys. Rev. D **82**, 083513 (2010).
[22] T. Konstandin and G. Servant, J. Cosmol. Astropart. Phys. 12 (2011) 009.
[23] P. Baratella, A. Pomarol, and F. Rompineve, J. High Energy Phys. 03 (2019) 100.
[24] K. Agashe, P. Du, M. Ekhterachian, S. Kumar, and R. Sundrum, J. High Energy Phys. 05 (2020) 086.
[25] K. Agashe, P. Du, M. Ekhterachian, S. Kumar, and R. Sundrum, J. High Energy Phys. 02 (2021) 051.
[26] F. R. Ares, M. Hindmarsh, C. Hoyos, and N. Jokela, J. High Energy Phys. 04 (2020) 100.
[27] N. Levi, T. Opferkuch, and D. Redigolo, J. High Energy Phys. 02 (2023) 125.
[28] R. K. Mishra and L. Randall, J. High Energy Phys. 12 (2023) 036.
[29] A. Kosowsky, M. S. Turner, and R. Watkins, Phys. Rev. Lett. **69**, 2026 (1992).
[30] A. Kosowsky, M. S. Turner, and R. Watkins, Phys. Rev. D **45**, 4514 (1992).
[31] A. Kosowsky and M. S. Turner, Phys. Rev. D **47**, 4372 (1993).
[32] M. Kamionkowski, A. Kosowsky, and M. S. Turner, Phys. Rev. D **49**, 2837 (1994).
[33] C. Caprini *et al.*, J. Cosmol. Astropart. Phys. 04 (2016) 001.
[34] C. Caprini *et al.*, J. Cosmol. Astropart. Phys. 03 (2020) 024.
[35] R. Caldwell *et al.*, Gen. Relativ. Gravit. **54**, 156 (2022).
[36] P. Auclair *et al.* (LISA Cosmology Working Group), Living Rev. Relativity **26**, 5 (2023).
[37] G. Agazie *et al.* (NANOGrav Collaboration), Astrophys. J. Lett. **951**, L8 (2023).
[38] J. Antoniadis *et al.*, arXiv:2306.16214.
[39] A. G. Riess *et al.*, Astrophys. J. Lett. **934**, L7 (2022).
[40] N. Aghanim *et al.* (Planck Collaboration), Astron. Astrophys. **641**, A6 (2020); **652**, C4(E) (2021).
[41] N. Schöneberg, G. Franco Abellán, A. Pérez Sánchez, S. J. Witte, V. Poulin, and J. Lesgourgues, Phys. Rep. **984**, 1 (2022).
[42] C. Wetterich, Phys. Lett. B **594**, 17 (2004).
[43] M. Doran and G. Robbers, J. Cosmol. Astropart. Phys. 06 (2006) 026.
[44] V. Poulin, T. L. Smith, T. Karwal, and M. Kamionkowski, Phys. Rev. Lett. **122**, 221301 (2019).
[45] F. Niedermann and M. S. Sloth, Phys. Rev. D **103**, L041303 (2021).
[46] F. Niedermann and M. S. Sloth, Phys. Rev. D **102**, 063527 (2020).
[47] M. Kamionkowski and A. G. Riess, Annu. Rev. Nucl. Part. Sci. **73**, 153 (2023).
[48] F. Niedermann and M. S. Sloth, Phys. Rev. D **105**, 063509 (2022).
[49] K. Freese and M. W. Winkler, Phys. Rev. D **104**, 083533 (2021).
[50] A. Afzal *et al.* (NANOGrav Collaboration), Astrophys. J. Lett. **951**, L11 (2023).
[51] J. Antoniadis *et al.* (EPTA Collaboration), Astron. Astrophys. **678**, A50 (2023).
[52] D. J. Reardon *et al.*, Astrophys. J. Lett. **951**, L6 (2023).
[53] H. Xu *et al.*, Res. Astron. Astrophys. **23**, 075024 (2023).
[54] I. M. Bloch, C. Csáki, M. Geller, and T. Volansky, J. High Energy Phys. 12 (2020) 191.
[55] Y. Bai and M. Korwar, Phys. Rev. D **105**, 095015 (2022).
[56] M. Cielo, M. Escudero, G. Mangano, and O. Pisanti, Phys. Rev. D **108**, L121301 (2023).
[57] While previous studies have addressed the effect of a PT on curvature perturbations at a parametric level [58–60], including the "big-bubble problem" in inflationary models [61], they have not precisely determined the

magnitude of the power spectrum. The power spectrum computed in [62] in the context of chain inflation, which arises from the same physical origin as our work, is applied in a different context.
[58] K. Freese and M. W. Winkler, Phys. Rev. D **107**, 083522 (2023).
[59] K. Freese and M. W. Winkler, Phys. Rev. D **106**, 103523 (2022).
[60] J. Liu, L. Bian, R.-G. Cai, Z.-K. Guo, and S.-J. Wang, Phys. Rev. Lett. **130**, 051001 (2023).
[61] E. J. Copeland, A. R. Liddle, D. H. Lyth, E. D. Stewart, and D. Wands, Phys. Rev. D **49**, 6410 (1994).
[62] M. W. Winkler and K. Freese, Phys. Rev. D **103**, 043511 (2021).
[63] P. Athron, C. Balázs, A. Fowlie, L. Morris, and L. Wu, Prog. Part. Nucl. Phys. **135**, 104094 (2024).
[64] C. J. Hogan, Phys. Lett. **133B**, 172 (1983).
[65] K. Enqvist, J. Ignatius, K. Kajantie, and K. Rummukainen, Phys. Rev. D **45**, 3415 (1992).
[66] M. Hindmarsh, S. J. Huber, K. Rummukainen, and D. J. Weir, Phys. Rev. D **92**, 123009 (2015).
[67] See Supplemental Material at http://link.aps.org/supplemental/10.1103/PhysRevLett.133.211003 for the calculation of the power spectrum of the phase transition time, which includes Refs. [68,69].
[68] R. Jinno and M. Takimoto, J. Cosmol. Astropart. Phys. 01 (2019) 060.
[69] R. Jinno and M. Takimoto, Phys. Rev. D **95**, 024009 (2017).
[70] T. Papanikolaou, V. Vennin, and D. Langlois, J. Cosmol. Astropart. Phys. 03 (2021) 053.
[71] G. Domènech, C. Lin, and M. Sasaki, J. Cosmol. Astropart. Phys. 04 (2021) 062; 11 (2021) E01.
[72] N. Ramberg, W. Ratzinger, and P. Schwaller, J. Cosmol. Astropart. Phys. 02 (2023) 039.
[73] Y. Akrami *et al.* (Planck Collaboration), Astron. Astrophys. **641**, A10 (2020).
[74] This conversion is not instantaneous in general. As the critical bubbles expand, they get acted upon by friction from the surrounding plasma and could reach a terminal velocity. For a supercooled PT, on the other hand, thermal effects are subdominant, and the runaway bubbles eventually collide and percolate; see [33,63,75] for reviews. However, exactly how the percolation takes place is not important for $\xi \ll 1$ and all we need to know is that through bubble percolation ρ_F is converted into $\tilde{\rho}_{\rm DR}$.
[75] D. J. Weir, Phil. Trans. R. Soc. A **376**, 20170126 (2018); **381**, 20230212(E) (2023).
[76] J. Garcia-Bellido and D. Wands, Phys. Rev. D **53**, 5437 (1996).
[77] D. Wands, K. A. Malik, D. H. Lyth, and A. R. Liddle, Phys. Rev. D **62**, 043527 (2000).
[78] K. A. Malik and D. Wands, Phys. Rep. **475**, 1 (2009).
[79] D. Langlois, F. Vernizzi, and D. Wands, J. Cosmol. Astropart. Phys. 12 (2008) 004.
[80] S. Ghosh, S. Kumar, and Y. Tsai, J. Cosmol. Astropart. Phys. 05 (2022) 014.
[81] W. Hu and N. Sugiyama, Astrophys. J. **471**, 542 (1996).
[82] S. Dodelson, *Modern Cosmology* (Academic Press, Elsevier Science, London, 2003).
[83] S. Bird, H. V. Peiris, M. Viel, and L. Verde, Mon. Not. R. Astron. Soc. **413**, 1717 (2011).
[84] H. A. Clark, G. F. Lewis, and P. Scott, Mon. Not. R. Astron. Soc. **456**, 1394 (2016); **464**, 2468(E) (2017).
[85] H. A. Clark, G. F. Lewis, and P. Scott, Mon. Not. R. Astron. Soc. **456**, 1402 (2016); **464**, 955(E) (2017).
[86] D. J. Fixsen and J. C. Mather, Astrophys. J. **581**, 817 (2002).
[87] P. Ade *et al.* (Simons Observatory Collaboration), J. Cosmol. Astropart. Phys. 02 (2019) 056.
[88] K. N. Abazajian *et al.* (CMB-S4 Collaboration), arXiv:1610.02743.
[89] J. Chluba, R. Khatri, and R. A. Sunyaev, Mon. Not. R. Astron. Soc. **425**, 1129 (2012).
[90] V. S. H. Lee, A. Mitridate, T. Trickle, and K. M. Zurek, J. High Energy Phys. 06 (2021) 028.
[91] T.-H. Yeh, J. Shelton, K. A. Olive, and B. D. Fields, J. Cosmol. Astropart. Phys. 10 (2022) 046.
[92] J. Chluba, A. L. Erickcek, and I. Ben-Dayan, Astrophys. J. **758**, 76 (2012).
[93] D. Hooper, A. Ireland, G. Krnjaic, and A. Stebbins, J. Cosmol. Astropart. Phys. 04 (2024) 021.
[94] J. C. Mather *et al.*, Astrophys. J. **420**, 439 (1994).
[95] D. J. Fixsen, E. S. Cheng, J. M. Gales, J. C. Mather, R. A. Shafer, and E. L. Wright, Astrophys. J. **473**, 576 (1996).
[96] Ref. [60] assumes the spatial energy density perturbation directly equals $\alpha_{\rm PT} f_{\rm DR} (\beta/H_{\rm PT})^{-5/2}$, omitting the numerical prefactor derived in the Supplemental Material. Their procedure in deriving $\mathcal{P}_\zeta(k)$ is also sensitive to the choice of a window function, while ours is not. Instead, our analysis derives $\mathcal{P}_\zeta(k)$ by starting with the primordial fluctuations and following the energy-momentum conservation equation for linear perturbations [78]. This could explain why our bounds differ.
[97] J. Chluba *et al.*, Bull. Am. Astron. Soc. **51**, 184 (2019).
[98] G. Franciolini, D. Racco, and F. Rompineve, Phys. Rev. Lett. **132**, 081001 (2024).
[99] J. Chluba, J. Hamann, and S. P. Patil, Int. J. Mod. Phys. D **24**, 1530023 (2015).
[100] S. Kasuya and M. Kawasaki, Phys. Rev. D **80**, 023516 (2009).
[101] M. Kawasaki, N. Kitajima, and T. T. Yanagida, Phys. Rev. D **87**, 063519 (2013).
[102] D. J. H. Chung and S. C. Tadepalli, Phys. Rev. D **105**, 123511 (2022).
[103] R. Ebadi, S. Kumar, A. McCune, H. Tai, and L.-T. Wang, Phys. Rev. D **109**, 083519 (2024).